

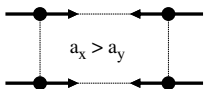
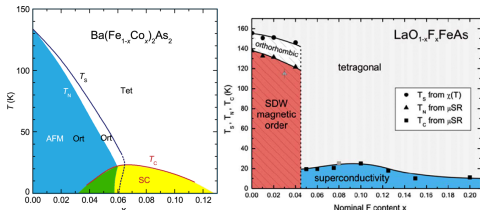
# Nematic state of the pnictides induced by the interplay between the spin, orbital, and lattice degrees of freedom

Shuhua Liang<sup>1,2</sup>, Adriana Moreo<sup>1,2</sup>, Elbio Dagotto<sup>1,2</sup>

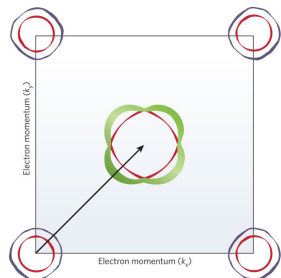
<sup>1</sup>Department of Physics and Astronomy, The University of Tennessee, USA  
<sup>2</sup>Materials Science and Technology Division, Oak Ridge National Laboratory

September 2, 2013

# Introduction: Iron based superconductor

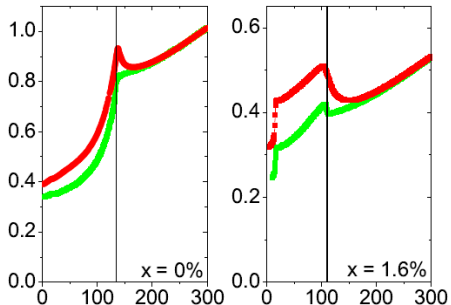


- $(\pi, 0)$  magnetic order.
- Orthorhombic lattice distortion.
- Bad metal!



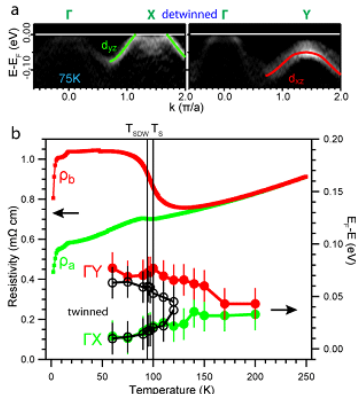
- Fermi Surface nesting and  $s+/-$  pairing have been proposed to explain results.  
*(Mazin et al., Kuroki et al., Graser et al.)*

# In-Plane Resistivity Anisotropy of $\text{BaFe}_2\text{As}_2$



- Resistivity along AF direction is smaller than that along the FM direction with a  $(\pi, 0)$  magnetic order.

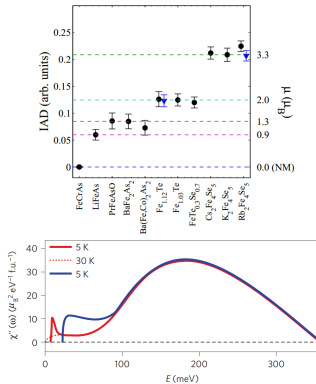
J-H. Chu *et al.*, Science 329, 824 (2010).



- Anisotropic band dispersion
- Fermi-surface: mostly xz.

Ming Yi *et al.*, PNAS. 108(17), 6878 (2011).

# Local moments

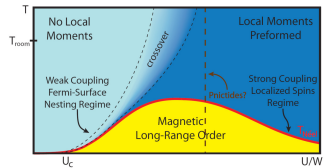
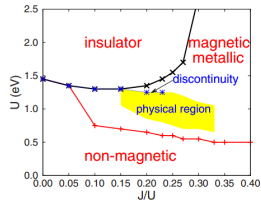


## ■ X-ray emission spectroscopy.

H. Gretarsson *et al.*, PRB **84**, 100509 (2011)

## ■ Neutron experiment: Large fluctuating moment from high-energy spin excitations.

M. Liu *et al.*, Nat. Phys. **8**, 376 (2012).



## ■ HF: similar phase diagrams with different models.

Q. Luo *et al.*, PRB **82**, 104508 (2010).

## ■ Intermediate coupling region.

P. Dai *et al.*, Nat. Phys. **8**, 709 (2012).

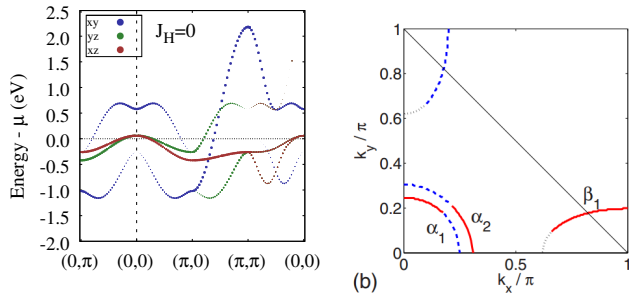
# Three Orbital Spin-Fermion Model

Spin-Fermion models for pnictides were introduced by  
W.-G. Yin, C. Lee, and W. Ku, PRL. **105**, 107004 (2010),  
W. Lv, F. Kruger, and P. Phillips, PRB **82**, 045125 (2010).

- Itinerant  $t_{2g}$  orbitals ( $xz, yz, xy$ ) coupled with the localized  $e_g$  orbitals ( $3z^2 - r^2, x^2 - y^2$ ) through Hund coupling.
- $J_{\text{Hund}} = 0.2\text{eV}$  ( $J/W \sim 0.1$ ) in agreement with HF.

$$\begin{aligned} H &= - \sum_{\langle ij \rangle}^{\sigma, \alpha, \beta} t_r^{\sigma, \alpha, \beta} (d_{i, \alpha, \sigma}^\dagger d_{j, \beta, \sigma} + H.c.) && \text{(Tight binding term)} \\ &+ \sum_{\langle ij \rangle} J_{\text{NN}} \vec{S}_i \cdot \vec{S}_j + \sum_{\langle ik \rangle} J_{\text{NNN}} \vec{S}_i \cdot \vec{S}_k && \text{(Heisenberg interaction)} \\ &- \sum_i J_{\text{Hund}} \vec{S}_i \cdot \vec{\sigma}_i && \text{(Hund interaction)} \end{aligned}$$

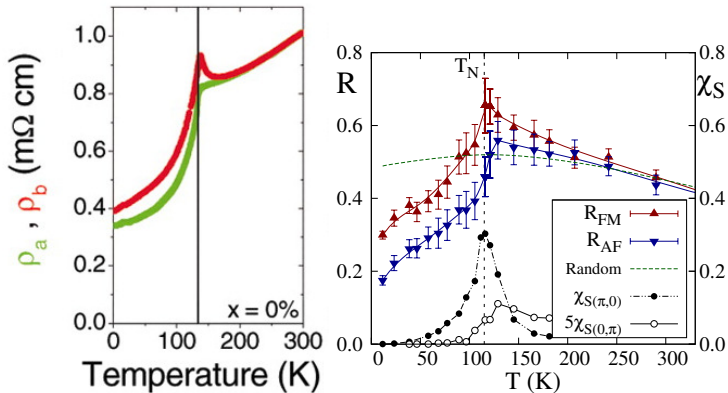
# Three Orbital Tight Binding Hamiltonian



- Hopping parameters were fitted to the LDA results.
- 2/3 filling (4 electrons per iron) was chosen to create the correct Fermi surface.

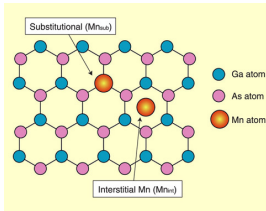
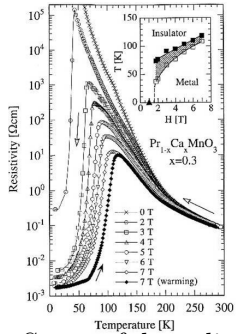
M. Daghofer, A. Nicholson, A. Moreo, and E. Dagotto, Phys. Rev. B **81**, 014511 (2010).

# Experimental results reproduced



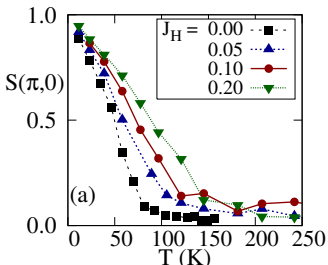
- The resistivity anisotropy with the metallic behavior.
- The resistivity peak at the critical temperature.

# The successful history of the spin-Fermion model



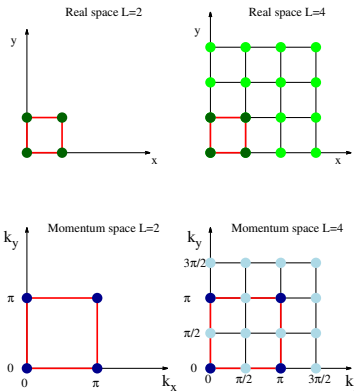
- Successful applications of the spin-Fermion model:  
Manganites, Cuprates, Diluted Magnetic Semiconductors,  
and the Heavy Fermions.
- Advantages of the spin-Fermion model:  
temperature dependent properties, phase transition, the  
inhomogeneity of the system, ...etc.

# New results: MC calculation in iron pnictides



- Based on CMR experience, we carried out a MC simulation in pnictides.
- Three  $t_{2g}$  orbitals are solved with exact diagonalization while local moments are solved through MC simulation.
- Strong Hund coupling enhances the  $(\pi, 0)$  magnetic order.
- 8000 MC steps were used for thermalization and 1,0000-100,000 steps for measurements at each temperature. Diagonalizations of the Hamiltonian reach as many as 10 million times at every temperature!

# Twisted Boundary Condition (TBC)

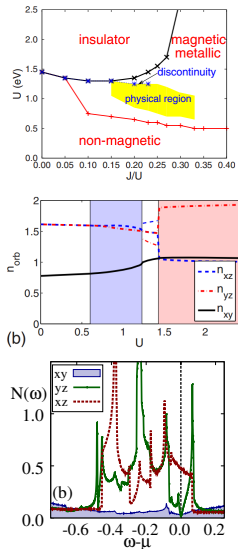


- Why twisted boundary condition?  
computer time  $\propto L^8$  !
- Add phases to the hopping parameters  
at the boundary of PBC lattice:  
 $t_{\text{TBC}} = t_{\text{PBC}} \cdot \exp(-i\Phi)$
- Phase  $\Phi$  changes from 0 to  $2\pi$ :  
simulating wave function with a wave  
length much larger than the lattice size.
- Fourier transform of observable:  
$$\begin{aligned} & \langle \tilde{\mathbf{O}}(\mathbf{k} - \frac{\Phi}{L})_{\text{TBC}} \rangle \\ &= \langle \exp\{i(\mathbf{k} - \frac{\Phi}{L}) \cdot \mathbf{r}\} \mathbf{O}(\mathbf{r}, \Phi) \rangle \end{aligned}$$

J. Salafranca, *et al.*, PRB **80**, 155133 (2009).

S. Liang *et al.*, PRL **109**, 047001 (2012).

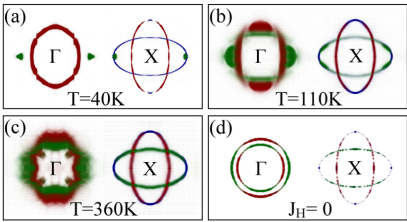
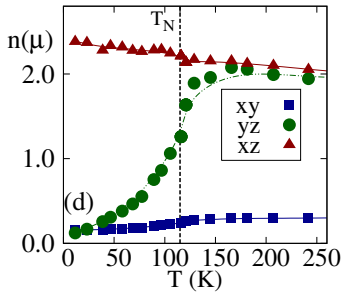
# Orbital Order and Fermi Surface Orbital Order



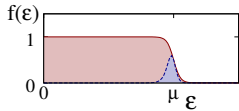
Spin fermion model gives similar results as mean field approximation (Q. Luo *et al.*, M. Daghofer, *et al.*):

- No “long range orbital order” in the physical regime.
- Ferro xz orbitally ordered  $(\pi, 0)$  C-AFM with strong interaction.
- Hund coupling opens a pseudo-gap for the  $yz$  orbital at the Fermi energy.
- Ferro xz Fermi surface orbital order, in agreement with the polarized ARPES

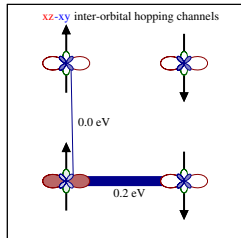
# Orbital Order at the Fermi Energy



- Below  $T_N$ ,  $\Gamma$  hole pocket is  $xz$  dominated.
- At  $T_N = 110K$ , symmetric  $xz$  satellite features arises near to the  $\Gamma$  hole pocket.
- Conducting electrons:  $n(\mu) = \frac{\beta e^{\beta(\epsilon-\mu)}}{(1+e^{\beta(\epsilon-\mu)})^2}$



# Resistivity Anisotropy along the FM and AF Directions



$\alpha\beta$	11	22	33	12	13	<b>xz-xy</b>	23
$D_x^{\alpha\beta}$	0.019	-0.003	0.073	0.013	0.125	0.005	
$D_y^{\alpha\beta}$	0.020	0.002	0.087	0.014	-0.01	0.011	

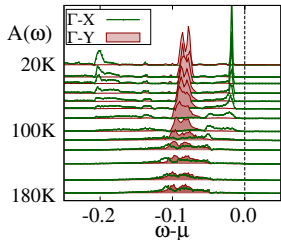
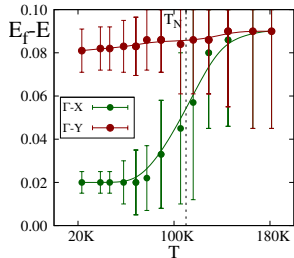
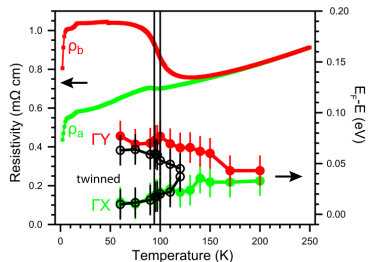
$$t_{xz \leftrightarrow xy}^x > t_{xz \leftrightarrow xy}^y$$

- $(\pi, 0)$  order creates strong ferro **xz** Fermi surface orbital order!
- Zero  $t_x^{yz,xy}$ ,  $t_y^{xz,xy}$  due to the symmetry of the As atoms.
- Drude weight through xz-xy along the x direction dominates all channels, tested with various models.

X. Zhang and E. Dagotto, PRB **84**, 132505 (2011).

S. Liang, *et al.*, PRL **109**, 047001 (2012).

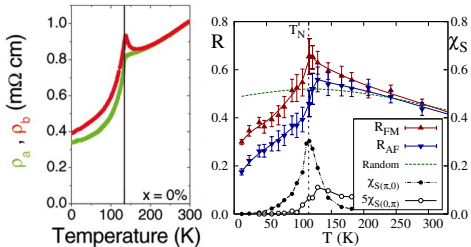
# Orbital Order at the Fermi Energy



- Compare  $\mathbf{A}(\mathbf{k}, \omega)$  of  $\text{yz}$  orbital at  $(\pi/2, 0)$  and  $\text{xz}$  orbital at  $(0, \pi/2)$ .
- Energy gap caused by Fermi surface orbital order is produced through MC simulations.

Ming Yi *et al.*, PNAS. **108(17)**, 6878 (2011).  
S. Liang, *et al.* in preparation.

# MC Temperature Dependence Curves of Resistivity

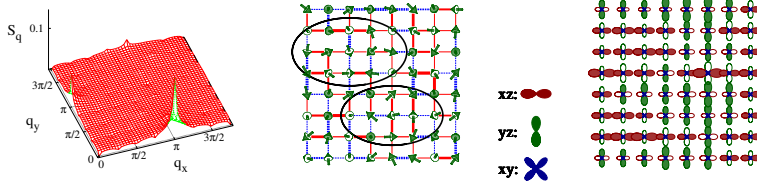


- Introduce anisotropy  $Jx/Jy = 1.14$  to simulate the strain.
- Near  $T_N$ , the MC measured resistivity is larger than that with random configurations (green dash lines).
- **What causes the resistivity peak at  $T_N$ ?**

R.M. Fernandes *et al.*, PRL. **107**, 217002 (2011).

S. Liang *et al.*, PRL **109**, 047001 (2012).

# Short Range Spin and Fermi Surface Orbital Order

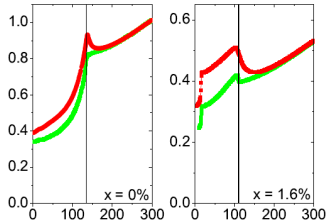


- At  $T_N$  coexisting  $(\pi, 0)$  and  $(0, \pi)$  magnetic order in both momentum space spin structure factor and real space spin configurations.
- The  $C - AFM$  patchy state with different orientations leads to corresponding short range Fermi Surface orbital order: **xz** favored or **yz** favored.
- Short range order leads to large resistivity.

R.M. Fernandes *et al.*, PRL **107**, 217002 (2011).

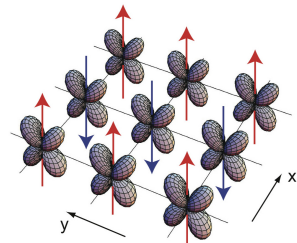
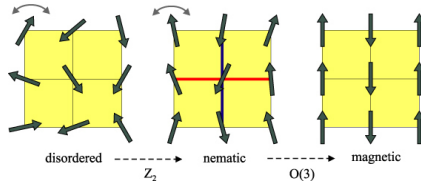
S. Liang *et al.*, PRL **109**, 047001 (2012).

# More Questions!



- What causes the anisotropy above  $T_N$ ?

# Magnetic Driven or Orbital Driven?



- Above  $T_N$ , the lattice distortion and the orbital order are stabilized by the nematic order.
- Ferro orbital order drives the structural transition and the magnetic order follows it.

R. M. Fernandes *et al.*, PRB **85**, 024534 (2012).

C.-C. Lee, W.-G. Yin, and W. Ku, PRL **103**, 267001 (2009).

C.-C. Chen *et al.*, PRB **80**, 180418(R) (2009).

W. Lv, F. Kruger, and P. Phillips, PRB **80**, 224506 (2009).

H. Kontani, T. Saito, and S. Onari, PRB **84**, 024528 (2011).

W. C. Lee, and P. W. Phillips, PRB **86**, 245113 (2012).

# What about the lattice?

- $\delta = \frac{(a_x - a_y)}{(a_x + a_y)} \sim 0.003$ .
- Is the orthorhombic lattice distortion strong enough to produce the anisotropy observed in R and spectral orbital weight?
- $\lambda \sim 0.2$ . Small but not negligible!

L. Boeri, *et al.*, PRL **101**, 026403 (2008).

H. Kontani, *et al.*, PRB **84**, 024528 (2011).

# New model: with lattice degree of freedom

- $R_0$  :  $Fe - As$  bond length at equilibrium.
- Lattice constructed with a tetrahedral structure at equilibrium.
- Elastic energy:

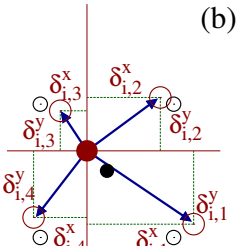
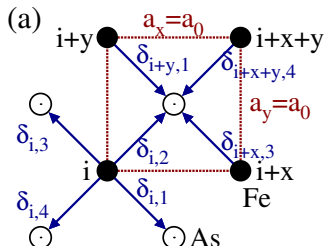


$$H_{elastic} = \frac{1}{2}k \sum_i \sum_{\nu=1}^4 (|\mathbf{R}_{Fe-As}^{i\nu}| - R_0)^2$$

- The ions are moving **collectively**, different from J-T distortion!

S. Liang *et al.*, PRL 111, 047004 (2013).

# New model: with lattice degree of freedom



- Lattice distortion:  $\epsilon_i = \frac{1}{4\sqrt{2}} \sum_{\nu=1}^4 (|\delta_{i,\nu}^y| - |\delta_{i,\nu}^x|)$ .
- Nematic magnetic order:  $\Psi_i = \mathbf{S}_i \cdot \mathbf{S}_{i+x} - \mathbf{S}_i \cdot \mathbf{S}_{i+y}$
- Quadrupole operator:  $O_{x^2-y^2} = n_{i,xz} - n_{i,yz}$
- Spin-lattice interaction:  
 $H_{\text{spin-lattice}} = -\tilde{g} \sum_i \epsilon_i \Psi_i$
- Electron-phonon interaction:  
 $H_{\text{orbital-lattice}} = \tilde{\lambda} \sum_i \epsilon_i O_{x^2-y^2}$

H. Kontani, T. Saito, and S. Onari, PRB **84**, 024528 (2011).

R.M. Fernandes, and J. Schmalian, Supercond. Sci. Technol. **25**, 084005 (2012).

S. Liang *et al.*, PRL **111**, 047004 (2013).

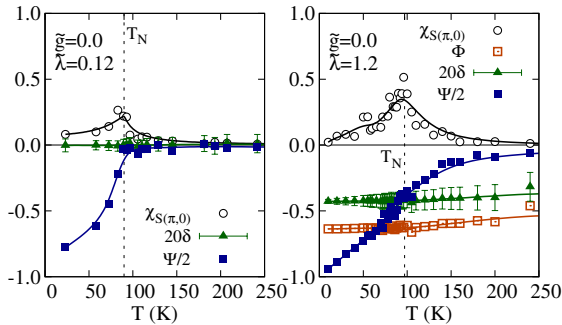
# New Hamiltonian with the lattice degree of freedom

- Spin, lattice, and orbitals are coupled in a way that the Hamiltonian is rotationally invariant.

$$\begin{aligned} H = & - \sum_{\langle ij \rangle} t_r^{\sigma, \alpha, \beta} (d_{i, \alpha, \sigma}^\dagger d_{j, \beta, \sigma} + H.c.) && \text{(Tight binding term)} \\ & + \sum_{\langle ij \rangle} J_{NN} \vec{S}_i \cdot \vec{S}_j + \sum_{\langle ik \rangle} J_{NNN} \vec{S}_i \cdot \vec{S}_k && \text{(Heisenberg interaction)} \\ & - \sum_i J_{\text{Hund}} \vec{S}_i \cdot \vec{\sigma}_i && \text{(Hund interaction)} \\ & + \tilde{\lambda} \sum_{\mathbf{i}} \epsilon_{\mathbf{i}} O_{x^2-y^2} && \text{(Orbital-lattice coupling)} \\ & - \tilde{g} \sum_{\mathbf{i}} \epsilon_{\mathbf{i}} \Psi_i && \text{(Spin-lattice coupling)} \\ & + H_{\text{elastic}} \end{aligned}$$

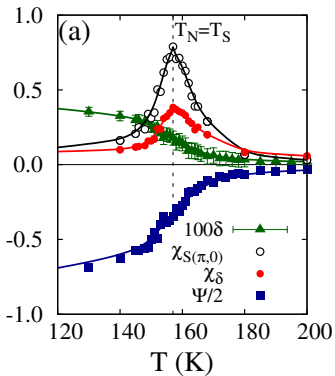
S. Liang *et al.*, PRL 111, 047004 (2013).

# New results with only $H_{\text{orbital-lattice}}$



- With only the orbital-lattice coupling ( $\tilde{\lambda} = 0.12$ ), no lattice distortion is observed.
- The fermi surface intra-orbital nesting favors the wrong lattice distortion.

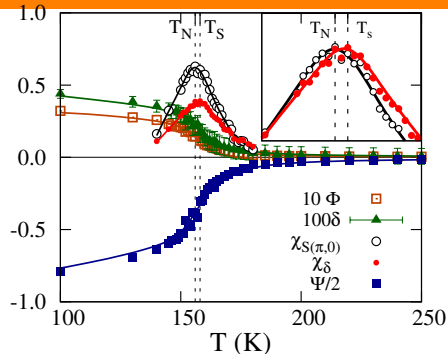
# New results with only $\mathbf{H}_{\text{spin-lattice}}$



- With only the spin-lattice coupling,  $\mathbf{T}_N=\mathbf{T}_S$ .
- $\tilde{g} = 0.16$ ,  $\tilde{\lambda} = 0$ , Lattice distortion  $\delta = (a_x - a_y)/(a_x + a_y) \approx 0.003$ .
- No orbital order is observed.

S. Liang *et al.*, PRL 111, 047004 (2013).

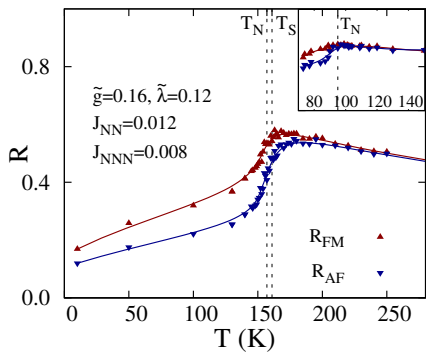
# $T_S > T_N$ with $H_{\text{orbital-lattice}}$ and $H_{\text{spin-lattice}}$



- Electron-phonon interaction ( $\tilde{\lambda} = 0.12$ ) pushes  $T_S$  above  $T_N$  upon the nematic magnetic order induced by the spin-lattice interaction ( $\tilde{g} = 0.16$ ).
- Weak ferro xz orbital order.

S. Liang *et al.*, PRL 111, 047004 (2013).

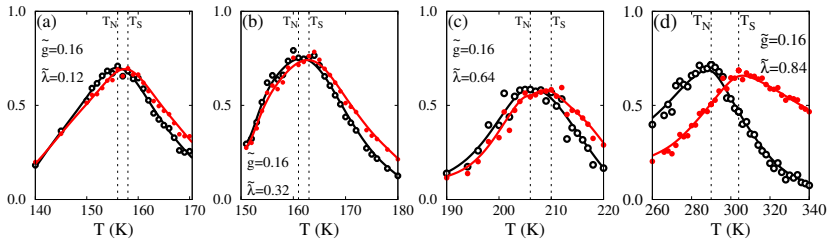
# $T_S > T_N$ with $H_{\text{orbital-lattice}}$ and $H_{\text{spin-lattice}}$



- Resistivity anisotropy and the band anisotropy reproduced above  $T_N$  without strain ( $\mathbf{J_x} = \mathbf{J_y}$ ).
- Without  $H_{\text{orbital-lattice}}$  and  $H_{\text{spin-lattice}}$ , no anisotropy observed above  $T_N$ .

S. Liang *et al.*, PRL 111, 047004 (2013).

# Separation between $T_N$ and $T_S$



■ The lattice susceptibility:

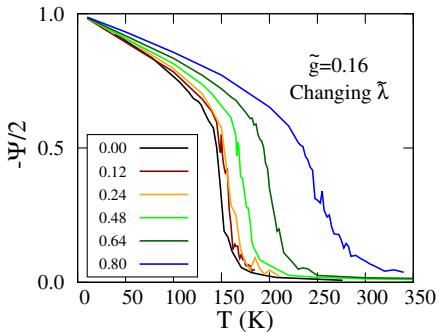
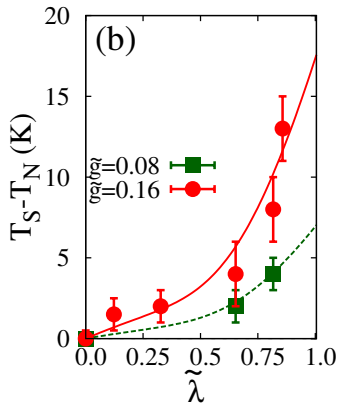
$$\chi_a = N\beta\langle\delta - \langle\delta\rangle\rangle^2, \text{ where } \delta = \frac{(a_x - a_y)}{(a_x + a_y)}.$$

■ The magnetic susceptibility:

$$\chi_{S(\pi,0)} = N\beta\langle S(\pi,0) - \langle S(\pi,0)\rangle\rangle^2.$$

S. Liang *et al.*, PRL 111, 047004 (2013).

# $T_S > T_N$ with $H_{\text{orbital-lattice}}$ and $H_{\text{spin-lattice}}$

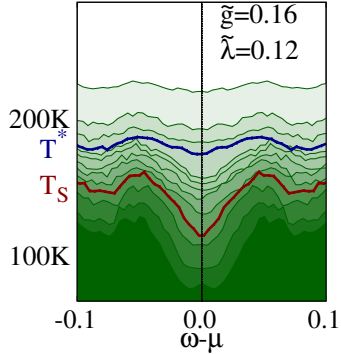
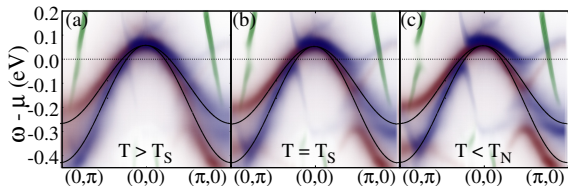


- When  $\tilde{\lambda} = 0$ ,  $T_N = T_S$ .
- Large  $\tilde{\lambda}$  enhances the separation between the  $T_N$  and the  $T_S$ .

- $T_N = T_S$ : First order transition, ( $\tilde{\lambda} = 0$ ).
- $T_N < T_S$ : Second order transition, ( $\tilde{\lambda} > 0$ ).

S. Liang *et al.*, PRL **111**, 047004 (2013).  
 R. M. Fernandes *et al.*, PRB **85**, 024534 (2012).

# Band splitting between xz and yz orbitals at $T_S$



- New results:  
Pseudo-gap appears above the  $T_S$ .
- Question:  
Short range magnetic order persists above  $T_S$ ?

S. Liang *et al.*, PRL 111, 047004 (2013).  
S. Liang *et al.* in preparation.

# Summary

- We developed a model including the lattice degree of freedom which is coupled to the local magnetic order and local orbital order.
- $H_{spin-lattice}$  is crucial to develop the orthorhombic distortion but not sufficient to stabilize the orbital order nor the higher  $T_S$ .
- $H_{orbital-lattice}$  determines the  $T_S - T_N$  and the order of the transition.
- The resistivity anisotropy and the band anisotropy are reproduced above  $T_N$ , although the Hamiltonian is rotationally invariant.
- Future work: Why pseudo-gap above  $T_S$ ? How do impurity and doping affect the results?

# Dimensionless parameters $\tilde{\lambda}$ and $\tilde{g}$

- $\tilde{\lambda} = \frac{\lambda}{\sqrt{kt}} = \frac{2\lambda}{\sqrt{kW}},$   
 $t \approx W/4, W \approx 3 \text{ eV}$   
 $\tilde{\lambda} \subset [0.0, 1.2]$
- $\tilde{g} = \frac{g}{\sqrt{kt}} = \frac{2g}{\sqrt{kW}},$   
 $\tilde{g} \subset [0.0, 1.0]$

Three  $\tilde{g}$  values are used: 0.0, 0.08 ,and, 0.16.

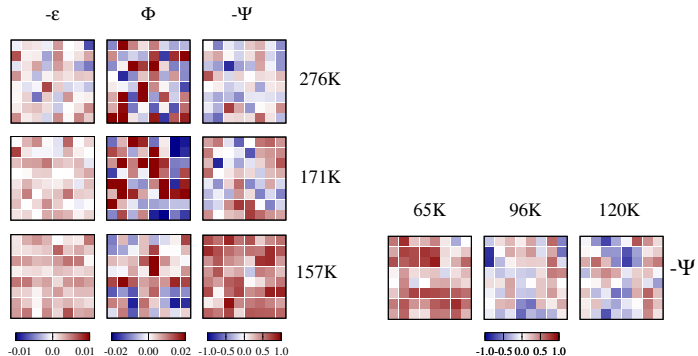
A.J. Millis *et al.*, PRL **77**, 175 (1996).

L. Boeri, *et al.*, PRL. **101**, 026403 (2008).

H. Kontani, *et al.*, PRB **84**, 024528 (2011).

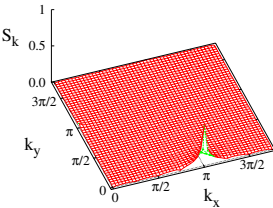
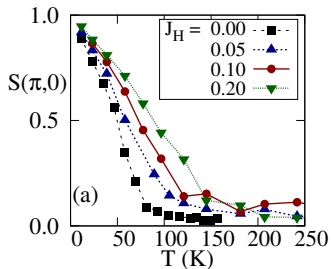
H. Kontani *et al.*, Solid State Comm. **152**, 718 (2012).

# MC snapshots



S. Liang, G. Alvarez, C. Sen, A. Moreo, and E. Dagotto, PRL **109**, 047001 (2012).  
S. Liang, A. Moreo, and E. Dagotto, in preparation.

# New results: MC calculation in the undoped limit

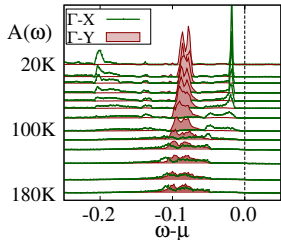
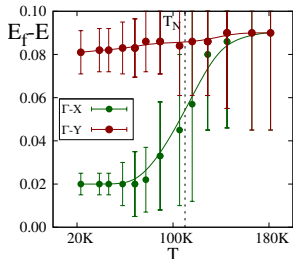
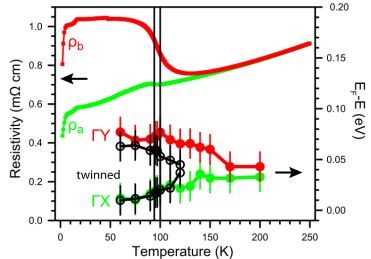


- Three  $t_{2g}$  orbitals are solved with exact diagonalization while local moments are solved through MC simulation.
- Heisenberg coupling  $J_{NNN}/J_{NN} = 2/3$
- Stronger Hund coupling enhances the  $(\pi, 0)$  magnetic order.

M. Daghofer *et al.*, Phys. Rev. B 81, 180514(R) (2010).

S. Liang, G. Alvarez, C. Sen, A. Moreo, and E. Dagotto, PRL

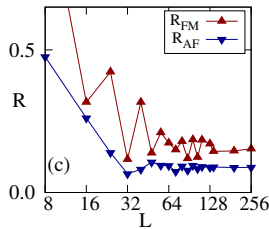
# Orbital Order at the Fermi Energy



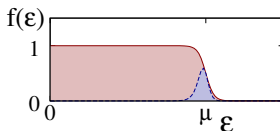
- Compare  $\mathbf{A}(\mathbf{k}, \omega)$  of  $\text{yz}$  orbital at  $(\pi/2, 0)$  and  $\text{xz}$  orbital at  $(0, \pi/2)$ .
- Energy gap caused by Fermi surface orbital order is produced through MC simulations.

Ming Yi *et al.*, PNAS. **108(17)**, 6878 (2011).  
S. Liang, *et al.*, PRL (2013).

# Resistivity Anisotropy along the FM and AF Directions



- DC Conductance (in  $\hbar/e^2$  units)  
 $= \sum_{l,m} |\langle \psi_l | \hat{V} | \psi_m \rangle|^2 \cdot \frac{f_l - f_m}{\epsilon_l - \epsilon_m} \cdot \delta(\epsilon_l - \epsilon_m)$
- Velocity matrix:  
 $i\hbar \hat{V}_{\hat{r}} = \sum_{\sigma,\alpha,\beta} \sum_{i,\hat{r}} t_{i,\hat{r},\sigma,\beta}^{\sigma,\alpha,\beta} (d_{i+\hat{r},\sigma,\beta}^\dagger d_{i,\sigma,\alpha} - d_{i,\sigma,\alpha}^\dagger d_{i+\hat{r},\sigma,\beta})$

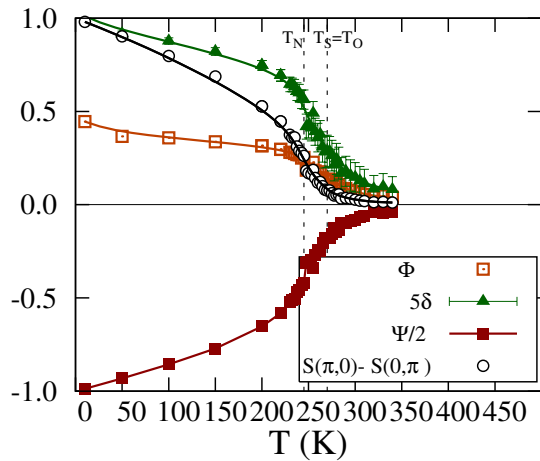


- Conducting electrons:  
 $n(\mu) = \frac{\beta e^{\beta(\epsilon-\mu)}}{(1+e^{\beta(\epsilon-\mu)})^2}$

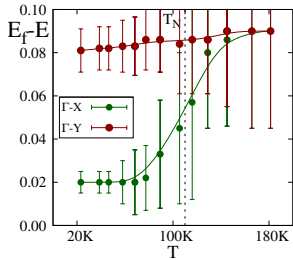
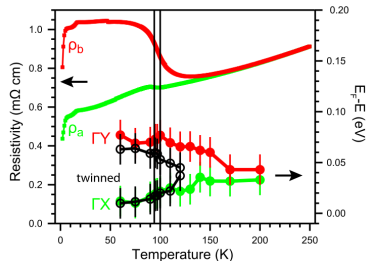
J. A. Verges, Comput. Phys. Commun. **118**, 71 (1999).  
X. Zhang and E. Dagotto, PRB **84**, 132505 (2011).

S. Liang *et al.*, PRL **111**, 047004 (2013).

$$T_S > T_N$$



# Gap between two bands



- Compare  $\mathbf{A}(\mathbf{k}, \omega)$  of **yz** orbital at  $(\pi/2, 0)$  and **xz** orbital at  $(0, \pi/2)$ .
- Energy gap caused by Fermi surface orbital order is produced through MC simulations.

Ming Yi *et al.*, PNAS. **108(17)**, 6878 (2011).

S. Liang, *et al.* in preparation.